

Overview of the ASACUSA program

Ryugo S. Hayano^a

^aDepartment of Physics, University of Tokyo,
7-3-1 Hongo, Bunkyo-ku, Tokyo 113-0033, Japan

The current and future program of ASACUSA (atomic spectroscopy and collisions using slow antiprotons) at CERN AD are presented, with an emphasis on the spectroscopy aspect of the collaboration. In the first half, the laser spectroscopy of an antiprotonic helium ($\bar{p}\text{He}^+$) atom, a neutral three-body Coulomb system consisting of an antiproton, a helium nucleus and an electron, with which we have achieved the best baryonic CPT constraint of $|m_{\bar{p}} - m_p|/m_p < 10^{-8}$, is discussed. Our plan to measure the ground-state hyperfine splitting of antihydrogen is dealt with in the second half.

1 Introduction

The name of our collaboration, ASACUSA, stands for atomic spectroscopy and collisions using slow antiprotons. As the name shows, our goal is to develop very low energy antiproton beams at CERN's antiproton decelerator (AD), and use them to study collision phenomena involving antiprotons, and also to carry out precise spectroscopy of exotic atoms containing antiproton.

The “collision” aspect of our collaboration was already discussed by Kuroda [1] at this conference. Therefore, in my talk, I will concentrate on the “spectroscopy” aspect of ASACUSA. Testing CPT invariance to highest-possible precision by ‘weighing antiprotons’ is one of the goals of ASACUSA. We have so far used antiprotonic helium atoms, an exotic three-body metastable atom consisting of an antiproton, an electron and a helium nucleus for this purpose. This will be the subject of the first half of my talk. After the 18-months shutdown of AD in 2005, we will start working on the ground-state hyperfine splitting spectroscopy of antihydrogen, which I will discuss in the second half.

2 Antiprotonic helium atoms

2.1 Its remarkable features

Antiprotonic helium atom (hereafter denoted $\bar{p}\text{He}^+$) is a naturally-occurring antiproton trap that has the following remarkable features [2]:

The atom can ‘store’ an antiproton for more than a microsecond. This ‘longevity’ occurs when the antiproton occupies a near-circular orbit having a large $n(\sim 38)$ and also large $\ell(\gtrsim 35)$. Unlike antihydrogen, it is not at all difficult to make $\bar{p}\text{He}^+$. Just stop antiprotons in a helium target. Then, about 3% of the stopped antiprotons automatically become trapped in the metastable states.

We usually use low-temperature ($T \sim 10$ K) helium gas as the target. The $\bar{p}\text{He}^+$ atoms that are produced collide with the surrounding helium atoms, and are thermalized. Therefore, the antiprotonic helium atoms are already cold. The Doppler width for a typical single-photon transition is about 500 MHz.

Fig. 1 shows an energy level diagram of $\bar{p}^4\text{He}^+$. The levels indicated by the continuous lines have metastable ($\gtrsim 1 \mu\text{s}$) lifetimes and deexcite radiatively, while the levels shown by wavy lines are short lived ($\lesssim 10$ ns) and deexcite by Auger transitions to antiprotonic helium ion states (shown by dotted lines). Since the ionic states are hydrogenic, Stark collisions quickly induce antiproton annihilation on the helium nucleus, as indicated in Fig. 1.

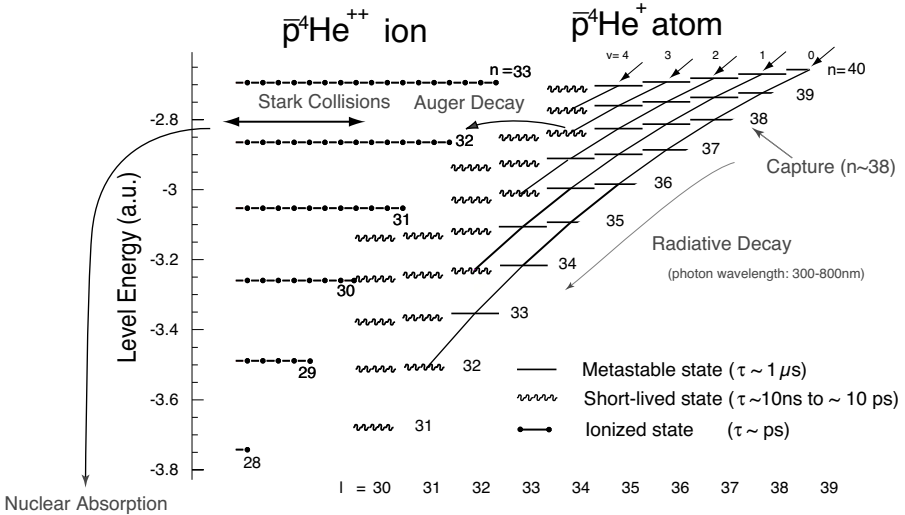


Figure 1: Level diagram of $\bar{p}\text{He}^+$ in relation to that of $\bar{p}\text{He}^{++}$. The solid and wavy bars stand for metastable and short-lived states, respectively, and the dotted lines are for l -degenerate ionized states.

2.2 Progress of the antiprotonic helium laser spectroscopy

Laser spectroscopy of $\bar{p}\text{He}^+$ works as follows: As shown in Fig. 1, there is a boundary between metastable states and short-lived states. For example, $(n, \ell) = (39, 35)$ is metastable, while $(n, \ell) = (38, 34)$, which can be reached from $(39, 35)$ by an $E1$ transition, is short lived. Thus, if we use a laser ($\lambda = 597$ nm in this particular case) to induce a transition from $(39, 35)$ to $(38, 34)$, (and of course if an antiproton happens to be occupying the $(39, 35)$ level at the time of laser ignition), the antiproton is deexcited to the short-lived state, which then Auger-decays to an ionic $(n_i, \ell_i) = (32, 31)$ state within $\lesssim 10$ ns. The ionic state is then quickly (usually within \sim ps) destroyed by Stark collisions, leading to the nuclear absorption/annihilation of the antiproton. Adding all these together, we expect to see a sharp increase in the \bar{p} annihilation rate in coincidence with the laser pulse. We measure the intensity of the laser-induced annihilation spike as a function of laser detuning, and compare the resonance-peak centroid ν_{exp} with the results of three-body QED calculations ν_{th} (calculated assuming $m_p = m_{\bar{p}}$ and $Q_p = -Q_{\bar{p}}$). See Fig. 2. So far, no statistically-significant deviation has been found. From this fact, we have concluded that 1) the three-body QED calculations have been performed with sufficient accuracy, and that 2) CPT holds within the experimental (and theoretical) error bars.

Our first experiment carried out in 1993 [3] at LEAR had a precision of about 50 ppm (5×10^{-5}). Theoretical predictions on the other hand scattered within about 1000 ppm. A breakthrough was made in 1995 by Korobov's first non-relativistic calculation, which improved the accuracy to some 50 ppm [4]. This was then improved to some 0.5 ppm by including relativistic corrections [5]. The precision of theoretical calculations continued to improve, and they have now reached $\lesssim 10^{-8}$ [6, 7].

In competition, experimental error bars also continued to decrease. After the first success, we soon found out that although $\bar{p}\text{He}^+$ atoms are fairly stable against frequent collisions with helium atoms, the collisions induce frequency shift and broadening of the resonance lines [8]. By measuring the resonance centroids at different helium densities and by extrapolating to zero density, we reached a precision of 60 ppb in 2001 [9]. This was the first physics result from the whole AD community.

Recently, we constructed a radio-frequency quadrupole decelerator (RFQD) [10] with which we can now decelerate the 5.3 MeV antiprotons extracted from AD to some 100 keV. This makes it possible to stop antiprotons in a very low density gas target ($\sim 10^{16-18}$ atoms/cm³), eliminating the need for the zero-density extrapolation. Figure 2 shows the present status of the experiment-theory comparison for seven transitions in $\bar{p}^4\text{He}^+$ (left) and six transitions in $\bar{p}^3\text{He}^+$ (right) [11]. Experimental errors include the absolute-frequency calibration uncertainties, and are typically $\sim \pm 100$ ppb. The theoretical predictions of Korobov (squares) [6] and Kino (triangles) [7] are mostly in the experimental error bars, but for some transitions there are discrepancies of ~ 100 ppb between the two. These differences do not yet affect the final CPT limits, but as the experimental precisions are improved, they may eventually become the dominant error source in the CPT limits deduced from $\bar{p}\text{He}^+$ spectroscopy.

Our measurements, which yield $\sim m_{\bar{p}}Q_{\bar{p}}^2$, are then combined with the (more precise) antiproton vs proton cyclotron frequency comparison done by the TRAP group at LEAR

[14]. This now provides the most stringent mass ($|m_{\bar{p}} - m_p|/m_p$) and charge ($|Q_{\bar{p}} + Q_p|/Q_p$) comparison between antiproton and proton of 10^{-8} , as listed in the Review of Particle Physics [15].

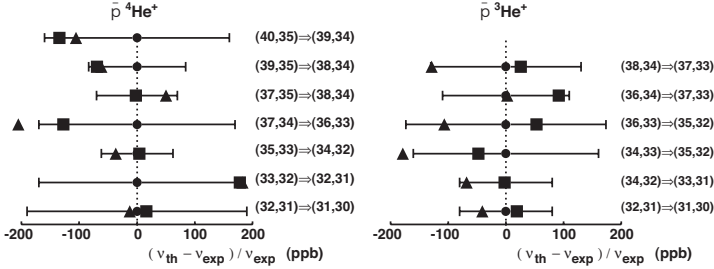


Figure 2: Comparisons between experimental result ν_{exp} (filled circles with errors) and theoretical predictions ν_{th} obtained assuming $m_p = m_{\bar{p}}$ and $Q_p = -Q_{\bar{p}}$ (squares [6] and triangles [7]). Taken from [11].

2.3 Discovery of metastable antiprotonic helium ions

Let us go back again to Fig. 1 and consider the fate of $\bar{p}\text{He}^{++}$ ions at very low target densities. The destruction of the $\bar{p}\text{He}^{++}$ states usually takes place in a matter of picoseconds due to the Stark collisions. If the $\bar{p}\text{He}^{++}$ ion is isolated in a vacuum, there are no collisions, and hence the $\bar{p}\text{He}^{++}$ states should become metastable (the radiative lifetimes of the circular states around $n_i \sim 30$ is several hundred ns). We, therefore, expect the prolongation of $\bar{p}\text{He}^{++}$ lifetimes at very low target densities.

This is exactly what we recently observed. In the left panel of Fig. 3, we show the annihilation spike produced by inducing the $\bar{p}^4\text{He}^+$ transition $(n, \ell) = (39, 35) \rightarrow (38, 34)$ measured by using the RFQD-decelerated beam at a low target density of 2×10^{18} atom/cm³. At this density, the decay time constant of the laser spike is still consistent with the Auger lifetime of the $(38, 34)$ level. However, as shown in the right panel, the shape of the laser-induced spike changes drastically in an ultra-low target density of 3×10^{16} atoms/cm³. Lifetime prolongation was also observed in the case of antiprotonic helium 3 ions. Systematic measurements of the ion lifetimes at various target densities have been carried out, which showed that the ionic-level lifetimes get shorter for larger principal quantum numbers. [12]

The long-lived antiprotonic helium ions $\bar{p}^4\text{He}^{++}$ and $\bar{p}^3\text{He}^{++}$ are quite interesting, since these are two-body systems and hence are practically free from theoretical errors. This motivates us to perform the laser spectroscopy of $\bar{p}\text{He}^{++}$. In principle, this appears possible, since we found that there is up to $\sim 50\%$ lifetime difference between the $\bar{p}\text{He}^{++}$ levels when the principle quantum number of the ion n_i is changed by one unit [12].

Hence, if we use a laser to produce an ionic state, and then use *another* laser (in the UV region) to induce transitions between n_i and $n_{i\pm 1}$, we should be able to observe a slight

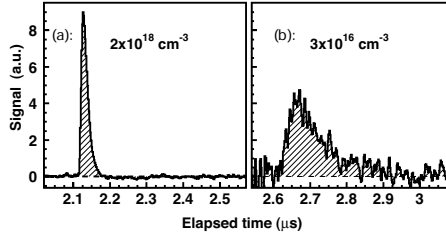


Figure 3: Annihilation spike produced by inducing the $\bar{p}\text{He}^+$ transition $(n, \ell) = (39, 35) \rightarrow (38, 34)$, measured at a high target density (a). A prolongation of the tail is observed at ultra-low densities (b), indicating the formation of long-lived $\bar{p}\text{He}^{++}$ ions.

change in the decay time constant of the laser spike (such as in Fig. 3(b)). This is by no means an easy measurement, but is nevertheless an important one.

2.4 Testing CPT or measuring a fundamental constant?

In 2004, we started a new series of measurements with a pulse-amplified continuous-wave (CW) laser system, in which the CW laser is stabilized and locked to an optical frequency comb [13]. Preliminary analyses look very promising, suggesting that we are likely to reach \sim ppb precision soon (in order to achieve this, we need continuing efforts of the theory community, so that the existing differences of some 100 ppb in the transition-frequency calculations are diminished).

In this way, the spectroscopy of $\bar{p}\text{He}^+$ is likely to play a leading role in baryonic CPT tests for some more time, but we will not be able to use $\bar{p}\text{He}^+$ to test CPT symmetry when we reach sub-ppb precision (the proton mass precision, measured in atomic unit, being 4.6×10^{-10} [16]). It is nevertheless important to measure $\bar{p}\text{He}^+$ transition energies to the best of our ability (and also urge theorists to improve their calculations) since with the $\bar{p}\text{He}^+$ spectroscopy we may be able to determine $m_{\bar{p}}/m_e$ as good as or better than m_p/m_e . Note that the CODATA value of m_p/m_e moved as much as 2.8 ppb between 1998 and 2002. It is hence important to compare the $m_{\bar{p}}/m_e$ value with the CODATA value as an independent check. If we believe that CPT is not violated at the level of ppb, the $\bar{p}\text{He}^+$ spectroscopy may eventually contribute to the determination of a fundamental constant m_p/m_e .

3 Ground-state hyperfine splitting of antihydrogen

3.1 Motivation

ASACUSA is now investing heavily in the future ground-state hyperfine splitting (GS-HFS) measurement of antihydrogen. Since the ground state of antihydrogen has infinite

lifetime, its high precision spectroscopy will give unprecedented accuracies in terms of CPT symmetry tests. In the case of hydrogen, the ground-state hyperfine splitting (GS-HFS) frequency ν_{HF} has been measured in a classic series of experiments which began in the 1930's with relatively simple atomic beam experiments, and culminated with maser experiments in the early 1970s which ultimately achieved a relative precision of order 10^{-12} (the latter technique is unfortunately not applicable to antimatter).

The 1S ground state of hydrogen is split due to the interaction of electron spin \vec{S}_e and proton spin \vec{S}_p according to $\vec{F} = \vec{S}_e + \vec{S}_p$ with quantum numbers $F = 0, 1$ (total spin) and $M = -1, 0, 1$ (projection of F onto the magnetic field axis). The hyperfine splitting frequency between the $F = 0$ and $F = 1$ states ν_{HF} is given by the Fermi contact interaction, yielding

$$\nu_{\text{HF}} = \frac{16}{3} \left(\frac{M_p}{M_p + m_e} \right)^3 \frac{m_e \mu_p}{M_p \mu_N} \alpha^2 c \text{Ry} (1 + \delta_{\text{QED}} + \delta_{\text{Zemach}}),$$

which is a direct product of the electron magnetic moment and the proton magnetic moment (M_p, m_e denote proton and electron mass, c the speed of light, α the fine structure constant, and Ry the Rydberg constant). The QED correction δ_{QED} is due mostly to the anomalous electron g -factor and is of the order of 1000 ppm, while δ_{Zemach} is so-called the Zemach correction [17] which can be written as

$$\delta_{\text{Zemach}} = \frac{2Z\alpha m_e}{\pi^2} \int \frac{d^3q}{q^4} \left[\frac{G_E(-q^2)G_M(-q^2)}{1 + \kappa} - 1 \right],$$

where $G_E(-q^2)$ and $G_M(-q^2)$ are the electric and magnetic form factors of the proton, and κ its anomalous magnetic moment. The Zemach correction, which is of the order of 30 ppm, therefore contains both the magnetic and charge distribution of the proton.

The GS-HFS frequency of antihydrogen is hence proportional to the spin magnetic moment of the antiproton, $\vec{\mu}_{\bar{p}}$, which is experimentally known only at the level of 0.3%. Below the level of several ppm accuracy, ν_{HF} also depends on the electric and magnetic form factors of the antiproton. The measurements of $\nu_{\text{HF}}(\bar{\text{H}})$ to a relative accuracy of better than 10^{-6} as discussed here will therefore yield an improvement of the value of $\vec{\mu}_{\bar{p}}$ by three orders of magnitude, and give some insight into the structure of the antiproton.

Furthermore, the only existing phenomenological extension of the standard model that includes CPT violations (the standard model extension – SME – of Kostelecky's group [18–22]) predicts that CPT violation in the 1S–2S transition is cancelled in first order, while for the hyperfine structure it is a leading-order effect. Although this model does not directly predict any CPT violation nor Lorentz invariance violation (LIV), it can be used as basis to compare CPT tests in different sectors, and as a guide where to look for possible CPT violating effects.

The SME-extension of the Dirac equation (for a free particle having a mass m) can be written as:

$$(i\gamma^\mu D_\mu - m - a_\mu \gamma^\mu - b_\mu \gamma_5 \gamma^\mu - \frac{1}{2} H_{\mu\nu} \sigma^{\mu\nu} + ic_{\mu\nu} \gamma^\mu D^\nu + id_{\mu\nu} \gamma_5 \gamma^\mu D^\nu) \psi = 0,$$

where γ_s, D_s, σ_s and ψ are as in the standard Dirac equations, a_μ and b_μ are the CPT (and Lorentz) violating parameters, while $H_{\mu\nu}, c_{\mu\nu}$ and $d_{\mu\nu}$ are Lorentz violating, but CPT

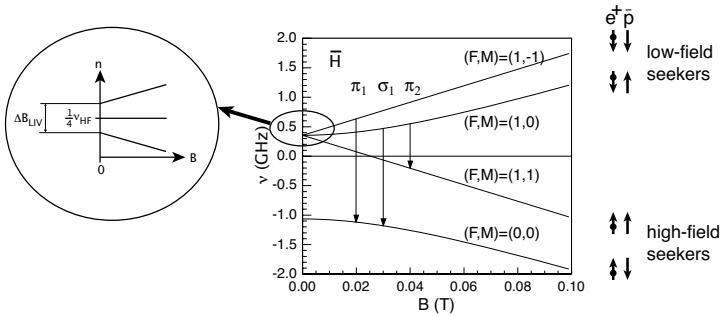


Figure 4: Right: Zeeman splitting of the ground state hyperfine levels of antihydrogen (Breit-Rabi diagram). The spin alignments of positron and antiproton in the high-field limit, when the spins are decoupled, is shown to the right. Left: Zero-field splitting of the $F = 1$ states in the presence of a CPT violating interaction as predicted by Bluhm et al. [22].

conserving parameters. The GS-HFS of antihydrogen is sensitive to the b_μ parameter [22] (also see Fig. 4).

Note that the CPT-violating parameters in SME have the dimension of energy (or frequency), hence it is advantageous to study CPT-violating effects in low-frequency transitions. Thus, within the SME framework, absolute energy (frequency) precision is important rather than relative precision $\delta\nu/\nu$. In other words, *within the framework of SME*, it is not necessary to measure the GS-HFS splitting to 18 digits (eventual goal of the 1S-2S laser spectroscopy) in order for the measurement to be competitive with the oft-quoted “most sensitive CPT bound” $|m_{K^0} - m_{\bar{K}^0}|/m_{\text{average}} < 10^{-18}$ [15]. This is because $|m_{K^0}c^2 - m_{\bar{K}^0}c^2|/h$ is constrained to $< 1.2 \times 10^5$ Hz in terms of frequency. The measurement of antihydrogen GS-HFS splitting to some 10^{-4} relative accuracy ($\Delta\nu \sim 100$ kHz) can thus already attain a sensitivity to the CPT-violating parameters as good as the $K^0 - \bar{K}^0$ comparison¹.

3.2 A possible method

We plan to apply a classical atomic beam method to the antihydrogen GS-HFS measurement [23]. The highest precision achieved for ordinary hydrogen using this method is $\delta\nu/\nu = 4 \times 10^{-8}$. If similar precision can be realized for antihydrogen, it will provide a more stringent test of the CPT symmetry than the $K^0 - \bar{K}^0$ mass difference. The atomic-beam measurement would involve:

1. An antihydrogen source - preferably a point-like source producing cold antihydro-

¹Note that the $K^0 - \bar{K}^0$ test (sensitive to the a parameter) and the $H - \bar{H}$ test (sensitive to the b parameter) cannot be directly compared; the purpose of the discussion here is to illustrate the order of magnitude of the achievable sensitivity to the CPT-violating parameters.

gens. The temperature should be as low as possible, but it is not necessary to produce < 1 K antihydrogen as would be required for antihydrogen trapping; a thermal source of some few tens of K would be sufficient.

2. A sextupole magnet line to focus the antihydrogen atoms.
3. A microwave cavity (1.4 GHz) to resonantly induce spin flip.
4. Another sextupole magnet to focus the spin-flipped antihydrogen.
5. An antihydrogen detector.

The proposed strategy is hence quite different from that proposed for the 1S-2S laser spectroscopy.

The atomic-beam method works best if the source is point like. A simulation, assuming a point-like source with a $T = 50$ K thermal distribution, and a sextupole beam line optimized for $v = 350$ m/s, shows that the beam line can transmit antihydrogen atoms within $\delta v = 25$ m/s FWHM, which in turn corresponds to a line width $\delta\nu/\nu$ of 1.56×10^{-6} . The transmission (solid angle and the velocity acceptance included) is about 10^{-4} . With a colder source of $T = 4.2$ K, the transmission will be increased by a factor 10, while with a much hotter source of $T = 150$ K the transmission goes down only by a factor 2. This shows that while a cold source is desirable, a relatively hot source is still tolerated. A relatively large source size of some 1 cm^3 of nested Penning traps, and technical difficulties to interface a sextupole beam line to a superconducting solenoid with a large-enough solid angle, lead us to consider alternative antihydrogen production methods. Therefore, within ASACUSA, two R&D efforts are being conducted.

One is to use a two-frequency Paul trap to simultaneously confine positrons (with a few GHz microwave) and antiprotons (with a few MHz radiofrequency) [23]. Such a trap, if realized, will produce antihydrogen atoms within a very small sphere ($< 1 \text{ mm}^3$). The trap will have openings to extract antihydrogen atoms with a large-enough solid angle, and will also have openings for lasers to deexcite antihydrogen atoms to the ground state. In fact, due to the alternating electric field whose strength increase linearly towards outside, antihydrogen atoms in high- n states are quickly dissociated and antiprotons and positrons are recycled. Only low-lying ($n \ll 10$) antihydrogen can leave the trap. This would ensure that only the ground-state antihydrogen atoms can reach the spin-analyzing cavity.

Alternatively, we are developing a so-called cusp trap (a pair of Helmholtz-like coils energized in opposite directions, combined with an octupole electric field) to simultaneously trap antiprotons and positrons and to synthesize antihydrogen atoms [24]. The source size realizable with this method is larger than the Paul-trap case, but the strong magnetic-field gradient at the antihydrogen extraction port can in principle produce a spin-polarized antihydrogen beam. This would make it possible to eliminate the first sextupole magnet, thereby achieving a larger solid angle.

These are both in the R&D phase, still requiring tests with protons and electrons to demonstrate that the concepts work. However, in view of the fact that the antihydrogen atoms produced in nested traps are rather hot and not necessarily in the ground state, we believe it is important that we pursue alternative production methods as discussed above.

This work was supported by the Grant-in-Aid for Specially Promoted Research (15002005) of MEXT Japan, the Hungarian Scientific Research Fund (OTKA T033079 and TeT-Jap-4/98), and the Japan Society for the Promotion of Science.

References

- [1] N. Kuroda, in these proceedings.
- [2] T. Yamazaki, N. Morita, R. S. Hayano, E. Widmann and J. Eades, *Physics Reports* **366**, 183 (2002).
- [3] N. Morita, M. Kumakura, T. Yamazaki, E. Widmann, H. Masuda, I. Sugai, R. S. Hayano, F. E. Maas, H. A. Torii, F. J. Hartmann, H. Daniel, T. von Egidy, B. Ketzer, W. Muller, W. Schmid, D. Horvath and J. Eades, *Phys. Rev. Lett.* **72**, 1180 (1994)
- [4] V.I. Korobov, *Phys. Rev. A* **54**, R1749 (1996).
- [5] V.I. Korobov and D.D. Bakalov, *Phys. Rev. Lett.* **79**, 3379 (1997).
- [6] V.I. Korobov, *Phys. Rev. A* **67**, 026501 (2003).
- [7] Y. Kino, M. Kamimura and H. Kudo, *Nucl. Instr. Methods B* **214**, 84 (2004).
- [8] H. A. Torii, R. S. Hayano, M. Hori, T. Ishikawa, N. Morita, M. Kumakura, I. Sugai, T. Yamazaki, B. Ketzer, F. J. Hartmann, T. Von Egidy, R. Pohl, C. Maierl, D. Horvath, J. Eades and E. Widmann, *Phys. Rev. A* **59**, 223 (1999).
- [9] M. Hori, J. Eades, R. S. Hayano, T. Ishikawa, J. Sakaguchi, E. Widmann, H. Yamaguchi, H. A. Torii, B. Juhasz, D. Horvath and T. Yamazaki, *Phys. Rev. Lett.* **87** 093401 (2001).
- [10] A. M. Lombardi, W. Pirkl and Y. Bylinsky, in *Proceedings of the 2001 Particle Accelerator Conference*, Chicago, 2001 (IEEE, Piscataway, NJ, 2001), pp. 585–587.
- [11] M. Hori, J. Eades, R. S. Hayano, T. Ishikawa, W. Pirkl, E. Widmann, H. Yamaguchi, H. A. Torii, B. Juhasz, D. Horvath and T. Yamazaki, *Phys. Rev. Lett.* **91** 123401 (2003).
- [12] M. Hori, J. Eades, R. S. Hayano, W. Pirkl, E. Widmann, H. Yamaguchi, H. A. Torii, B. Juhasz, D. Horvath, K. Suzuki, and T. Yamazaki, *Phys. Rev. Lett.* **94**, 063401 (2005).
- [13] J. Reichert, R. Holzwarth, Th. Udem and T. W. H[?]nsch, *Opt. Commun.* **172**, 59 (1999).
- [14] G. Gabrielse, A. Khabbaz, D. S. Hall, C. Heimann, H. Kalinowsky and W. Jhe , *Phys. Rev. Lett.* **82**, 3198 (1999).
- [15] S. Eidelman *et al.*, *Phys. Lett. B* **592**, 1 (2004).
- [16] P. J. Mohr and B. N. Taylor, to appear in *Review of Modern Physics* **76** (2004); also available on web at <http://physics.nist.gov/constants>.
- [17] J. R. Sapirstein and D. R. Yennie, in *Quantum Electrodynamics*, ed. T. Kinoshita, (World Scientific, Singapore), pp 560–672 (1990).
- [18] D. Colladay and V. A. Kostelecky, *Phys. Rev.* **D55**, 6760 (1997).
- [19] R. Bluhm, V. A. Kostelecky and N. Russell, *Phys. Rev. Lett.* **79**, 1432 (1997).
- [20] R. Bluhm, V. A. Kostelecky and N. Russell, *Phys. Rev.* **D57**, 3932 (1998).
- [21] V. A. Kostelecky, *Phys. Rev. Lett.* **80**, 1818 (1998).

- [22] R. Bluhm, V. A. Kostelecky and Neil Russell, Phys. Rev. Lett., **82**, 2252 (1999).
- [23] ASACUSA collaboration, CERN-SPSC 2005-02, available from CERN Document Server.
- [24] A. Mohri and Y. Yamazaki, Europhys. Lett. **63**, 207 (2003).